Preparing for the Emergence of a Highly Pathogenic Influenza Pandemic

Gregory A. Mohl[1], Mckay D. Jensen[1], Spencer K. Wallentine[2], Kelly L. McGuire[1], Roger G. Harrison PhD[2], David D. Busath MD[3]
Departments of [1]Physiology and Developmental Biology and [2]Chemistry and Biochemistry
Brigham Young University, Provo, UT

Introduction

The Influenza virus infects about 1 billion people worldwide and kills hundreds of thousands of people each year. The virus frequently mutates, making it a difficult target for antivirals. A mutation in a membrane protein, the M2 ion channel, causes the virus to be insensitive to Amantadine and Rimantadine. Neuraminidase inhibitors are also vulnerable to viral resistance.

We are working to develop new compounds that inhibit influenza A M2 in a unique, possibly irresistible way: i.e. metal complexes of traditional M2 blockers that could also complex (1,2) with the highly conserved selectivity-conferring His37 cluster. The compounds have been tested on M2 peptides reconstituted in liposomes and full-length M2 protein expressed in oocytes, and on viral infection of MDCK cell culture. Absorption spectroscopy was found to be a useful method of identifying metal-complex stability in different buffer solutions.

Methods & Materials

Compound Synthesis

Amantadine or cyclooctylamine were added to bromoacetic acid or 2-bromoacetamide and dissolved in solvent. The solution was made basic and then heated and stirred overnight. The desired acids or amides were isolated and characterized by MS, NMR and IR spectroscopy. To form the copper complexes, a copper(II) salt was added to a basic solution of ligand (NaH for the amides). Upon addition of copper a deep blue color formed. The copper complexes were isolated and characterized by MS, ICP-M, NMR and IR spectroscopy. Some were characterized by single crystal X-ray diffraction. The stability of each complex (100 μM) was tested by UV-vis spectrometry in several buffers.

Stability Assay

The test compounds were dissolved in an organic or aqueous solution. These solutions were diluted to 100 μM in the buffers used for the Oocyte and Mini-Plaque assays. The solutions were then monitored by UV-vis spectrophotometry for changes in peak shape and intensity over 72 hours.

Liposome Assay

Liposomes were prepared as described previously (2) from E. coli polar lipid with or without M2 peptide (0.1 mg peptide/20 mg lipid/ml 50 mM KCl, 50 mM K_2HPO_4, 50 mM KH_2PO_4, pH 6.0), and extruded (200 nm pores). M2 (22-62) peptide was A/Udorn/72, either WT or S31N. The liposome suspension was diluted 100-fold into 165 mM NaCl, 1.67 mM NaCitrate, 0.33 mM citric acid, pH 6.0. For tests of channel block, metal complex was added to 100 μM 2:00 minutes prior to the valinomycin-induced vesicle polarization, which drives influx of protons into the liposomes. Then, after CCCP-induced depolarization, back-titrations with HCl were used to normalize the initial valinomycin-induced pH changes in the buffer, allowing the calculation of proton uptake per (nominal) channel per second. Percent block relative to complex-free controls was calculated after corrections for background fluxes in protein free controls.

Oocyte Assay

Oocytes from Xenopus laevis (Ecocyte, Austin, TX) were maintained in ND-96^{++} solution (96 mM NaCl, 2 mM KCl, 1.8 mM CaCl2, 1mM MgCl2, 2.5 mM sodium pyruvate, 5 mM HEPES-NaOH, pH 7.4) at 17° C until injection of ~40 ng of A/Udorn/72, A/Udorn/72 S31N, or A/Udorn/72 S31N, H37A mRNA. After injection, the oocytes were maintained in ND96^{++} pH 7.4 until electrophysiological recording. 72 hrs after mRNA injection, whole-cell currents were recorded with a two-electrode voltage-clamp apparatus at Vm=-20 mV. Oocyte currents were recorded in standard Barth's solution (0.3 mM NaNO3, 0.71 mM CaCl2, 0.82 mM MgSO4, 1.0 mM KCl, 2.4 mM NaHCO3, 88 mM NaCl, 15.0 mM HEPES, pH 7.5. Inward proton current was induced by perfusion with Barth's pH 5.3. Percentage block of the original inward current by 100 μM test compound was measured just before washout, which was done 8:50 minutes after drug exposure for all compounds except where noted.

Viral Mini-Plaque Assay

As described previously (3), MDCK cells were seeded onto coverslips at 2.4×10^4 cells/vial in 1 ml of 5% FBS DMEM. The cells were incubated overnight at 37°C to form a monolayer. Then the medium was replaced with an aCSF solution (148 mM NaCl, 3 mM KCl, 1.6 mM $CaCl_2$*H_2O, 0.8 mM $MgCl_2$*$6H_2O$, 0.75 mM Na_2HPO_4*$7H_2O$, 0.1 mM NaH_2PO_4*H_2O, pH 7.2) with a test compound 2-50 μM and inoculated with 100μl of trypsinized influenza A virus, either A/CA/07/2009 (1100 PFU/ml), A/WS/33 (1200 PFU/ml), or A/Victoria/03/75 (700 PFU/ml), and incubated at 33* C for 16 hours. Each coverslip was then air-dried for 30 min and stained with FITC-labeled antibody for miniplaque counting. EC_{50}s were obtained by least-squares fit of a binding function in KaleidaGraph.

Cytotoxicity Assay

Using a previously described method (4), MDCK cells were seeded at 2×10^4 cells per well in 96-well plates in 5% FBS/DMEM, and incubated for 48 h (37* C, 5% CO_2). After replacing the growth medium with 100 μl 1% FBS/DMEM containing 1-9 two-fold dilutions of the 1 mM test compound the plates were sealed and incubated at 37* C in 5% CO_2 atmosphere for 72 h. Cells from six wells without compound treatment serve as negative controls. The wells were then rinsed, fixed, and stained with 50 μl of 0.03% crystal violet (w/v) in 20% methanol for 10 min. After washing, lysis buffer was added to elute the crystal violet and the optical density of individual wells was quantified spectrophotometrically at 620 nm. CC_{50}s were obtained by least-squared fit of a binding function in KaleidaGraph.

Results

Amantadine in M2 S31N

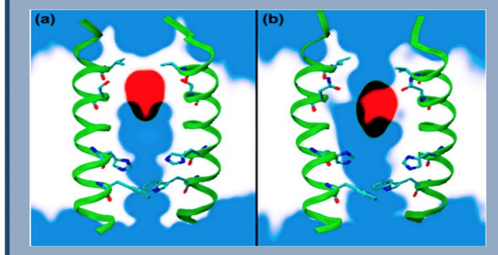

Figure 1:Molecular Dynamics Simulations of AMT in M2.
Left: AMT blocks the WT M2 channel. *Right:* In the S31N channel, AMT does not fully disrupt the water string (5). Subsequent umbrella sampling results also display reduced binding affinity (6).

Compound Structures

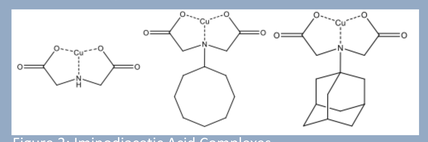

Figure 2: Iminodiacetic Acid Complexes
From left to right: Cu(IDA), Cu(CO-IDA), Cu(AMT-IDA)

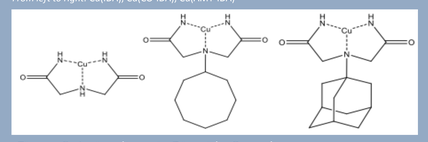

Figure 3: Iminodiacetic Diamide Complexes
From left to right: Cu(IDAA), Cu(CO-IDAA), Cu(AMT-IDAA)

Purity Analysis

Compound	Copper Content ICP-OES
Cu(IDA)•1.5H_2O	Theoretical: 28.7% Observed: 29.4%
Cu(IDAA)	ND
Cu(AMT-IDA) •2H_2O	Theoretical: 17.5% Observed: 15.2%
Cu(AMT-IDAA) •DMF•2H_2O	Theoretical: 15.3% Observed: 19.5%
Cu(CO-IDA) •H_2O•Acetate•Na	Theoretical: 15.7% Observed: 16.3%
Cu(CO-IDAA) •0.5DMF•2H_2O	Theoretical: 16.7% Observed: 15.7%

Figure 4: ICP-OES Purity Analysis
Purity of the compounds was assessed by ICP-OES. Elemental Analysis and NMR (not shown) were also used to determine compound purity.

Stability Assay

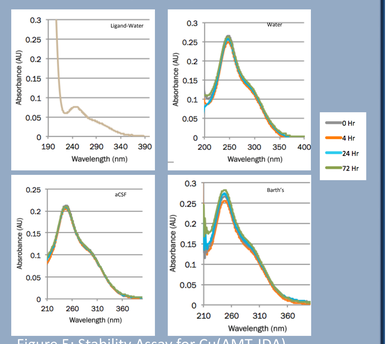

Figure 5: Stability Assay for Cu(AMT-IDA)
UV absorbance was measured at 0, 4, 24, and 72 hours after dissolving the compound in the buffer.

Liposome Assay

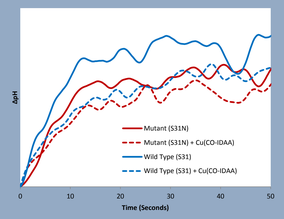

Figure 6: Potentiometric pH measurements of Cu(CO-IDAA) in Liposomes
The pH change due to protons flowing through M2 into liposomes immediately after adding valinomycin is plotted against time. Valinomycin transports potassium ions out of the liposomes, causing a voltage gradient over the liposome membrane. Protons then enter the liposomes through the M2 channel with an approximately exponential decay. The efficacy of an M2 blocker can be assessed by comparing the initial rates of the fitted proton flux through liposomes with and without the compound present. The exemplary traces in this figure (of n=3) indicate a block due to Cu(CO-IDAA) of about 20% in the mutant and about 40% in the wild type.

Oocyte Assay

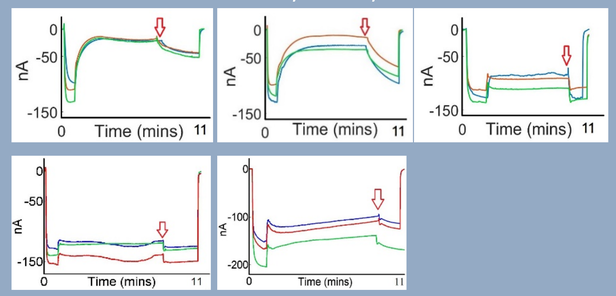

Figure 7: Membrane current traces for *Xenopus laevis* oocytes transfected with Udorn/72 M2 in TEVC
Top: *From left to right:* Traces of Cu(CO-IDAA) with Udorn/72 M2 S31N, WT, and H37A.
Bottom: *From left to right:* Traces of CO-IDAA with Udorn/72 M2 S31N and WT
At t=0, perfusion is switched to pH 5.3. At t=1 min, perfusion switches to same solution with 100μM of test compound. The 5-minute washout (no drug) is marked by the red arrow. Finally, the perfusion is returned to Barth's pH 7.4 to check cell viability.

MiniPlaque Assay

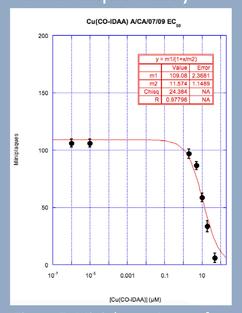

Figure 7: Miniplaque Assay of Cu(CO-IDAA) in A/CA/07/09
The number of miniplaques on the coverslip (n=4) is plotted against the concentration of test compound (μM).

Stability Assay

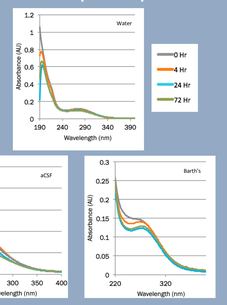

Figure 7: Stability Assay for Cu(CO-IDAA).
UV absorbance was measured at 0, 4, 24, and 72 hours after dissolving the compound in the buffer.

Mini-Plaque Assay EC_{50} (μM)

Strain	$CuCl_2$	Cu(IDA)	Cu(IDAA)	Cu(AMT-IDA)	Cu(AMT-IDAA)	Cu(CO-IDA)	Cu(CO-IDAA)
A/CA/07/09 (S31N)	3.8 ± 0.9	8.2 ± 2.0	4.4 ± 0.6	6.9 ± 1.2	4.9 ± 0.8	ND	11.6 ± 1.1
A/WS/33 (S31N)	4.3 ± 1.0	ND	ND	2.4 ± 0.3	4.1 ± 2.4	ND	2.3 ± 0.2
A/Victoria/75 (WT)	1.1 ± 0.3	ND	ND	4.2 ± 1.7	ND	ND	8.4 ± 0.7

Figure 12: EC_{50} of Drug Candidates Against Influenza A Virus in Mini-Plaques
The concentration of test compound (μM) at which 50% of infections were reduced, was determined for the metal complexes in three strains. The results suggest that the test compounds are effective in preventing infection. We consider 5 μM to be an acceptable EC_{50} for a useful therapeutic.

Cytotoxicity Assay CC_{50} (μM)

$CuCl_2$	Cu(IDA)	Cu(IDAA)	Cu(AMT-IDA)	Cu(AMT-IDAA)	Cu(CO-IDA)	Cu(CO-IDAA)
19.0 ± 3.6	115 ± 9	64 ± 6	64 ± 7	52 ± 5	147 ± 38	180 ± 15
	IDA	IDAA	AMT-IDA	AMT-IDAA	CO-IDA	CO-IDAA
	> 0.5 mM	> 1 mM	> 1 mM	> 1 mM	> 1 mM	258 ± 20

Figure 13: CC_{50} of Drug Candidates
The concentration of test compound (μM) at which 50% of cells were non-viable, was determined for the metal complexes and their corresponding ligands. The ligands alone were not toxic below 1mM, except for CO-IDAA. The copper complexes were more toxic, ranging from 52-180 μM. The preferred toxic concentration is at least 10 times greater than the EC_{50}. Most of the compounds are in this range.

Liposome Assay

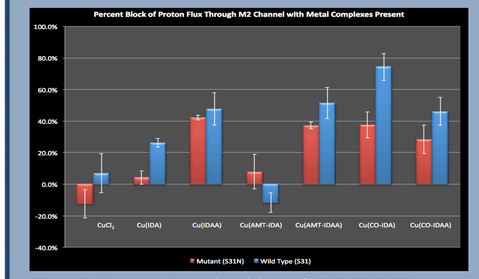

Figure 9: Liposome H^+-uptake inhibition for M2 22-62 WT or S31N
Percent block at 2:00 mins (i.e. fast block) after exposure to 100 μM metal complex is higher for metal complexes than for $CuCl_2$, which showed no inhibition of both S31N and WT. The fast block of the S31N peptide was comparable to that of WT for most compounds, suggesting their potential usefulness against modern AMT-resistant virus. Error bars are +/-SD (N=3, except for S31N $CuCl_2$ and S31N Cu(AMT-IDA) (N=6).

Oocyte Assay

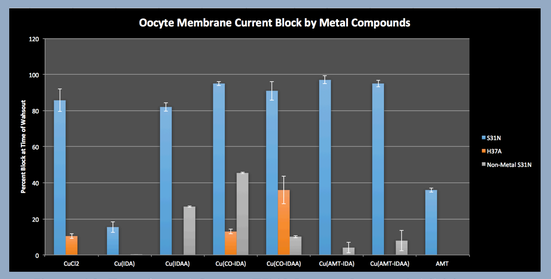

Figure 10: Transfected Oocyte TEVC Proton Current Inhibition
Percent Block at 8:50 mins (or 28:50 mins for Cu(CO-IDA) or 58:50 mins for Cu(AMT-IDA) by 100 μM metal complexes against A/Udorn/72 M2 S31N or A/Udorn/72 M2 (S31) H37A, contrasting with metal-free complexes. Complexation with ligands based on traditional M2 WT blockers, amantadine and cyclooctylamine is beneficial in the context of AMT-insensitive M2.

Conclusions

The potential disease burden of a highly pathogenic, antiviral-resistant, and emerging strain of the influenza virus underscores the need for an array of new antivirals to save lives in a pandemic situation. Vaccines are not useful in this situation because of the unpredictability of emerging strains and the time it takes to make and distribute vaccines on a large scale. Currently, the only antivirals that are approved for use will lose their efficacy as new mutant strains emerge with increased resistance. The M2 has been shown to be a promising drug target because of the highly conserved H37 residue in the TM domain, which is essential for proton conductance. Investigators searching for an M2 blocker for the S31N channel have been, with a few exceptions (8), unsuccessful to date. We have shown that these metal complexes are very effective in preventing infection in viral infectivity assays, even in two strains of the S31N mutant.

We have shown with liposome and oocyte assays that the copper complexes prevent proton flux in the M2 channel with much higher efficacy than the copper-free ligands. They are even more effective than copper chloride in blocking the channel. The ability to bind at the His-37 site, coupled with a large ligand that can fill the binding pocket, appears to provide long-term binding and disruption of the water string.

The cytotoxicity results show that the copper complexes were considerably less toxic to the cells than copper chloride. For example, Cu(CO-IDAA) was shown to be more than 9 times less toxic than $CuCl_2$. The ligand that is attached to the copper also seems to have an effect on how toxic the compound is. Hopefully, other variations of these compounds could be synthesized with yet lower toxicities without sacrificing the ability to block the channel.

This study shows that adding ligands to copper changes the toxicity of the compound and its ability to prevent infection.

References

1. Gandhi, C.S.; Shuck, K.; Lear, J.D.; Dieckmann, G.R.; DeGrado, W.F.; Lamb, R.A.; Pinto, L.H. Cu(II) Inhibition of the Proton Translocation Machinery of the Influenza A Virus M2 Protein. *J. of Biol. Chem.,* 1999, *274,* p. 5474-5482.

2. Gordon, N.; Divalent Copper Compounds as Inhibitory Agents of Influenza A. *Thesis*, **2014**.

3. Sharma, M.; Yi, M.; Dong, H.; Qi, H.; Peterson, P.; Busath, D.D.; Zhou, H.; Cross, T.A. Insight into the Mechanism of the Influenza A Proton Channel from a Structure in a Lipid Bilayer. *Science*, **2010**, *550*, p. 509-512

4. Kolocouris, Antonios; Tzitzoglaki, Christina; Johnson, F. Brent; Zell, Roland; Wright, Anna K.; Cross, Timothy A.; Tietjen, Ian; Fedida, David; Busath, David D. Aminoadamantanes with Persistent in Vitro Efficacy against H1N1 (2009) Influenza A. *J. Med. Chem.* **2014**, *57*, p. 4629-4639.

5. Schmidtke, M.; Schnittler, U.; Jahn, B.; Dahse, H.-M.; Stelzner, A. A rapid assay for evaluation of antiviral activity against coxsackie virus B3, influenza virus A, and herpes simplex virus type 1. *J. Virol. Methods* **2001**, *95*, 133-145.

6. Gleed, M.; Busath, D. Why bound amantadine fails to inhibit proton conductance according to simulations of the drug-resistant influenza A M2 (S31N). *J. Phys. Chem. B* **2015**, *119* , 1225-1231.

7. Gleed, M. L.; Ioannidis, H.; Kolocouris, A.; Busath, D. D. Resistance-mutation (N31) effects on drug orientation and channel hydration in amantadine-bound Influenza A M2. *J. Phys. Chem. B* **2006**, *119*, 11548-59.

8. Li, F.; Ma, C.; DeGrado, W. F.; Wang, J. Discovery of highly potent inhibitors targeting the predominant drug-resistant S31N mutant of the influenza A virus M2 proton channel. *J. Med. Chem*, **2016**, E-Pub Jan. 16.

Acknowledgements

The authors thank Dallin Gillete for preparations of mRNA and MacKenzie Hart for assistance with some miniplaque assays. This projects was supported by mentoring and stimulus funds from BYU as well as NIH R01 AI23007 to Dr. Timothy A. Cross, Florida State University.